

Loss of prostaglandin D₂ synthase: a key molecular event in the transition of a low-grade astrocytoma to an anaplastic astrocytoma

Cathy A. Payne,¹ Sanaz Maleki,¹
 Marinella Messina,¹ Maree G. O'Sullivan,⁵
 Glenn Stone,⁵ Nathan R. Hall,²
 Jonathon F. Parkinson,¹ Helen R. Wheeler,³
 Raymond J. Cook,⁴ Michael T. Biggs,⁴
 Nicholas S. Little,⁴ Charles Teo,⁶
 Bruce G. Robinson,^{1,7} and Kerrie L. McDonald^{1,7}

¹Hormones and Cancer Group, Cancer Genetics Laboratory, Kolling Institute of Medical Research; Departments of ²Anatomical Pathology, ³Medical Oncology, and ⁴Neurosurgery, Royal North Shore Hospital, St. Leonards, New South Wales, Australia; ⁵Commonwealth Scientific and Industrial Research Organization, Mathematical and Information Sciences, North Ryde, New South Wales, Australia; ⁶Neuroendoscopy: Centre for Minimally Invasive Neurosurgery, Prince of Wales Private Hospital, Randwick, New South Wales, Australia; and ⁷Faculty of Medicine, University of Sydney, New South Wales, Australia

Abstract

Reduction in the mRNA and protein expression of lipocalin-like prostaglandin D₂ (PGD₂) synthase (PGDS), the main arachidonic acid metabolite produced in neurons and glial cells of the central nervous system, is a significant biological event involved in the malignant progression of astrocytomas and is predictive of poor survival. *In vitro*, the addition of the main PGDS metabolite, PGD₂, to A172 glioblastoma cells devoid of PGDS resulted in antiproliferative activity and cell death. *In vitro* PGD₂ substitution also enhanced the efficacy of cyclo-oxygenase-2 inhibitors. This finding has exciting implications for early interventional efforts for the grade 2 and 3 astrocytomas. [Mol Cancer Ther 2008;7(10):3420–8]

Received 7/7/08; accepted 7/29/08.

Grant support: Cure for Life Foundation, Andrew Olle Memorial Trust, and Sydney Neuro-Oncology Group.

The costs of publication of this article were defrayed in part by the payment of page charges. This article must therefore be hereby marked *advertisement* in accordance with 18 U.S.C. Section 1734 solely to indicate this fact.

Note: Present address for J.F. Parkinson: Department of Neurosurgery, Prince of Wales Public Hospital, Randwick, New South Wales, Australia.

Requests for reprints: Kerrie L. McDonald, Hormones and Cancer Group, Cancer Genetics Laboratory, Kolling Institute of Medical Research, Reserve Road, St. Leonards, New South Wales, 2065 Australia. Phone: 61-2-99267176; Fax: 61-2-99268484. E-mail: kerriem@med.usyd.edu.au

Copyright © 2008 American Association for Cancer Research.

doi:10.1158/1535-7163.MCT-08-0629

Introduction

Glioblastoma multiforme (GBM) is a devastating disease with a bleak survival outlook of just 15 months. GBM typically arise *de novo*; however, around 10% of these tumors arise from earlier clinical diagnoses of WHO malignancy grade 2 (AII) and grade 3 (AIII; anaplastic) astrocytoma. Patients diagnosed with an AII have an average survival of 2 to 8 years compared with 2 years for a AIII (1). The marked individual survival variability that is associated with AII and AIII is strongly influenced by the dynamics of malignant progression. Careful management is critical to reduce the risk of the tumor progression.

Increasing age is a negative prognostic marker for all astrocytoma grades (2). However, no other validated factor has been identified that can unequivocally predict which AII will undergo malignant progression to an AIII and how soon this event will occur after diagnosis. Astrocytoma malignant progression was reported to be more rapid in patients with an AII containing more than 5% gemistocytes (3). However, other studies have shown no such correlation (4). Several genes such as *TP53* (5–7), *epidermal growth factor receptor* (8, 9), and *platelet-derived growth factor receptor* (10) have been associated with the tumorigenesis and anaplastic progression of human gliomas, but the prognostic significance of these genes has also been unclear. For example, positive *TP53* mutation status was found to be a significantly unfavorable predictor of survival but not p53 overexpression (5). However, some studies have found that *TP53* mutations only predict a shorter time interval before progression in patients with AII lesions (1).

Very few microarray studies have specifically profiled genes involved in the malignant transformation of an AII to an AIII. An early study compared AII samples with normal brain and identified six genes, which included *tissue inhibitor of metalloproteinase 3*, *epidermal growth factor receptor*, and *glia-derived neurite-promoting factor*, whose expression was heightened in 60% to 100% of AII specimens (11). In addition, *platelet-derived growth factor receptor- α* , *pleiotrophin*, and *secreted protein, acidic, cysteine rich (osteonectin)* were up-regulated by at least 2-fold in 20% to 60% of AII compared with the non-tumor brain samples. No comparison was made between AII and AIII specimens in this study. In a separate study, a tissue microarray was constructed using tissue from 130 astrocytomas (72 GBM, 49 AIII, and 9 AII; ref. 12). The activator protein-2 α transcription factor was shown to be absent in 99% and 98% of GBM and AIII, respectively, compared with AII and normal brain, all of which maintained expression of activator protein-2 α (12). Thus, activator protein-2 α expression correlated inversely with glioma grade.

In this study, we used microarray analysis and employed the multivariate analysis algorithms, SDDA and GeneRave (13), to identify significant gene differences initially between AII and AIII specimens. One significant gene change was identified by GeneRave, which was later identified as lipocalin-type prostaglandin D₂ (PGD₂) synthase (*PGDS*). In a larger cohort of astrocytic tumors (which included GBM), we report the loss of *PGDS* mRNA and protein expression in malignant astrocytomas but not in AII. The addition of PGD₂, a metabolite of *PGDS*, to a human A172 glioblastoma cell line that lacked endogenous *PGDS* mRNA and protein expression, resulted in the suppression of cell growth, and this response was augmented in the presence of cyclo-oxygenase-2 (COX-2) pathway inhibitors.

Materials and Methods

Tumor Sampling and Data Collection

A total of 98 patients with a newly diagnosed astrocytoma [WHO malignancy grade 2, 3, or 4 (GBM)] were selected from the Sydney Neuro-Oncology Group database and of which had undergone surgery at Royal North Shore Hospital or North Shore Private Hospital. A smaller group of patients diagnosed with AII were recruited from Prince of Wales Private Hospital. Approval for this study was obtained from the Human Research Ethics Committees of the participating institutions.

No patients received chemotherapy or radiotherapy before surgery. Surgically removed tumors were snap frozen in liquid nitrogen immediately and stored at -80°C until RNA extraction. Formalin-fixed, paraffin-embedded tumor blocks were provided by the Department of Anatomical Pathology, Royal North Shore Hospital.

Post-surgery, all GBM patients received radiation therapy, with the majority of these patients also receiving chemotherapy. Most of the patients diagnosed with an AIII received radiation therapy. Survival assessment was conducted in May 2008. Briefly, 8 patients were diagnosed as an AII, and of these, 1 patient had died (mean survival based on events, 8.22 years). Of the 24 patients diagnosed as AIII, 6 patients have died (mean survival, 7.61 years). GBM consisted of 66 patients, and of these, 59 patients have died (mean survival, 1.39 years).

Whereas paraffin tissue was available for all 98 patients, summarized above, frozen tissue was only available for 49 specimens (22 samples included in the microarray analysis and an additional 27 samples included in the quantitative PCR). For this current study, the initial microarray analysis was conducted on patients diagnosed with AII ($n = 5$) and AIII ($n = 6$) tumors only. After the gene of interest was discovered, the microarray analysis was extended to include GBM samples (AII, $n = 5$; AIII, $n = 6$; GBM, $n = 11$). The mRNA was validated using an independent set of tumors and included AII ($n = 5$), AIII ($n = 8$), and GBM ($n = 14$) specimens.

Microarray Data and Quantitative PCR

Total RNA was extracted from the frozen glioma samples using the Qiazol reagent (Qiagen) and processed as

described previously (13). Approximately 20 µg glioma RNA and 20 µg commercial total normal brain (Ambion) were labeled with Cy5 and Cy3 dyes, respectively, and hybridized to microarray slides printed with the Compugen 19,000 human oligonucleotide library (Adelaide Microarray Facility, University of Adelaide) using standard protocols. All samples were processed, scanned, and quality checked as described previously (13). The microarray data (ETABM-167) is deposited in the public database, ArrayExpress.⁸ For the analysis of gene expression measures, preprocessing of the data, including PrintTipLoess normalization, was carried out using the R statistical software (version 2.0.1) libraries contained within the Bioconductor open source software.⁹

To specifically examine genes that were differentially expressed between AII and AIII, multivariate analysis of the array data was done, as described previously, using two proprietary methods developed by the Commonwealth Scientific and Industrial Research Organization, GeneRave and SDDA (13). One gene, lipocalin-type *PGDS*, was identified to be significantly differentially expressed between the tumor grades.

To confirm *PGDS* mRNA expression levels, the different grades of astrocytoma were analyzed with quantitative PCR using TaqMan Gene Expression Assays (Applied Biosystems) as described previously (13). The expression levels of all tumor specimens were compared with a "normal reference," which comprised the average expression of 1 commercial total brain, 1 autopsy brain sample, and 1 human cortical neuronal cell line (HCN-1 α). Differential expression of the mRNA levels was assessed statistically using REST-XL (Relative Expression Software Tool, version 2), with which relative expression ratios are computed based on the PCR efficiency and crossing point differences. Student's *t* test analysis was used to evaluate the statistical significance of the mRNA expression levels of the target genes between the two groups (SPSS version 14.0 software; SPSS).

Immunohistochemical Staining

To assess protein expression levels of *PGDS* and COX-2, an enzyme that is responsible for the formation of prostanoids of which include prostaglandin, formalin-fixed, paraffin-embedded tissue was sectioned at 4 µm, placed onto *Superfrost* Ultra charged slides (Menzel-Glasser), and baked for 2 h at 65°C. Sections were cleared in xylene and rehydrated through graded ethanols and brought to water. The sections were heat retrieved in boiling waterbath for 20 min in modified citrate buffer (pH 6.0) for *PGDS* staining or Tris/EDTA (pH 9.0) for COX-2 staining and then allowed to slowly cool before being washed in commercial Tris-HCl (DAKO Australia). Peroxidase activity was quenched in 3% H₂O₂ for 5 min and then rinsed in buffer. A serum-free protein block (DAKO Australia) was used to block endogenous protein activity

⁸ <http://www.ebi.ac.uk/arrayexpress>

⁹ <http://www.bioconductor.org/>

for 10 min at room temperature. Rabbit polyclonal anti-human PDGS (Novus Biologicals) was run at 1:250 for 30 min at room temperature. Mouse monoclonal anti-human COX-2 (DAKO Australia) was run at 1:100 for 60 min at room temperature. Both antibodies had corresponding normal fraction IgG with matched primary concentrations on control tissue. All staining was done on an automated platform (DAKO Autostainer Plus; DAKO Australia). Complex was detected using Envision Flex+ horseradish peroxidase for 30 min at room temperature and visualized with 3,3'-diaminobenzidine chromagen (DAKO Australia), resulting in a brown insoluble precipitate. Sections were then counterstained in Harris hematoxylin, dehydrated through graded ethanols, cleared in xylene, and mounted. Immunostaining for PGDS and COX-2 was scored using the Allred scoring system (14), which takes into consideration the estimated proportion of positive staining (score of 0-5) and is added to a score of 0 to 3 for intensity of positive cells (total score range, 0-8). Gliomas that score ≤ 2 were generally regarded to be "negative" for PGDS.

Survival Analysis

Cox proportional hazards regression analysis was done to assess PGDS protein expression level as a prognostic indicator for survival adjusted for age. Kaplan-Meier survival analysis was used to generate survival curves and estimates of median survival times. The log-rank test was used to compare survival curves for samples split by age, tumor type, and PGDS expression. All statistical analyses were conducted using SPSS version 14.0 software (SPSS).

DNA Extraction

DNA was extracted from fresh frozen tissue using phenol-chloroform extraction methods as described previously (15) and from paraffin-embedded tissue using commercially available reagents (Genra Puregene DNA Purification Kit; Qiagen).

Mutation Analysis

Exons 1 to 6 of *PGDS* were sequenced for 18 GBM samples. Primer sequences are summarized in Supplementary Table S1.¹⁰ Sequencing was done by Sydney University Prince Alfred Molecular Analysis Centre using the ABI PRISM 3700 platform (Applied Biosystems).

Methylation Analysis

Bisulfite treatment of DNA from patients diagnosed with GBM ($n = 28$), GBM cell lines (A172 and T98G), and a normal brain cell line (HCN-1 α) were carried out using the MethylEasy DNA bisulfite modification kit according to the manufacturer's instructions and as described previously (ref. 15; Human Genetics Signatures). CpGenome universal methylated and unmethylated controls were included with each reaction (Chemicon International). Methylation status was assayed for *PGDS* using INA primers ordered through the "INA primer by design" service (Human Genetics

Signatures). The primers amplified a region of intron 1 of the *PGDS* gene and covered 32 CpG dinucleotides. Amplification was conducted using two rounds of PCR. The first round of amplification was conducted at 60°C and the second round of amplification was conducted at 67°C.

In vitro Studies

The human glioblastoma cell line A172 was obtained from the American Type Culture Collection, maintained in DMEM (Life Technologies/Invitrogen), and supplemented with 10% FCS in a humidified atmosphere containing 5% CO₂ at 37°C. RNA was extracted from the A172 cell line to assess endogenous *PGDS* mRNA levels using TRIzol according to the manufacturer's protocol (Invitrogen) and as described previously (16). Low *PGDS* mRNA expression levels were measured and confirmed using quantitative PCR as described earlier.

Exogenous Treatment of PGD₂ and COX-2 Inhibitors, Nimesulide and Etodolac, to A172 Cells

PGD₂ (Cayman Chemical) was reconstituted in DMSO and stored at -20°C. Dilutions were then prepared in DMEM supplemented with 10% FCS and added to A172 cell medium at a range of concentrations (1×10^{-4} – 1×10^{-10} mol/L). The PGD₂ concentration found to be optimal for cell experiments was 1×10^{-5} mol/L. The final concentration of 0.05% DMSO was added to cell medium for control cells. Both nimesulide and etodolac (Sigma-Aldrich) were reconstituted in ethanol (molecular grade 95%) and dilutions were prepared in DMEM as described for PGD₂ and added to A172 cell medium at a range of concentrations (2×10^{-4} – 5×10^{-5} mol/L). The optimal concentration for both nimesulide and etodolac was 5×10^{-5} mol/L.

To determine if PGDS expression is regulated by methylation, the demethylating agent 5-aza-deoxycytidine was dissolved in DMSO and diluted in culture medium for experiments. 5-Aza-deoxycytidine was used at 1×10^{-6} and 5×10^{-6} mol/L as described previously (17).

Growth Inhibition, Cell Viability, and Apoptosis Assays: MTS, Trypan Blue Exclusion, and TUNEL

Approximately 24 h before receiving the exogenous treatments, A172 cells were trypsinized and seeded in a 96-well microtiter plate at an optimized density of 5×10^3 per well. The treatments of PGD₂, COX-2 inhibitors, and demethylating agents were delivered to the cells 24 h post-cell seeding and this was referred to as day 0. The number of viable cells in proliferation was determined at three time points: day 1 (24 h), day 2 (48 h), and day 3 (72 h) using a colorimetric cell proliferation assay, referred to as the MTS assay (CellTiter 96 AQU_{EOUS} Non-Radioactive Cell Proliferation Assay; Promega). A hemocytometer-based trypan blue dye exclusion assay was also used to assess cell viability, where nonviable cells turn blue. Apoptosis was measured with the TUNEL stain (Boehringer Mannheim). The number of TUNEL-positive cells were counted in three low-power fields and expressed as a percentage. A minimum of three independent experiments were conducted for each cell treatment, with a minimum of three internal replications in each experiment.

¹⁰ Supplementary material for this article is available at Molecular Cancer Therapeutics Online (<http://mct.aacrjournals.org/>).

Results

PGDS Expression Is Lost within High-Grade Astrocytoma

Gliomas were grouped into *a priori* classes, AII and AIII, and underwent pairwise discrimination using both GeneRave and SDDA algorithms. One single gene, lipocalin-type *PGDS*, was identified by the GeneRave algorithm to discriminate AII from AIII. The predictive accuracy of *PGDS* to separate the two groups was 80%. By plotting the gene expression values of the astrocytomas, the scatter plot shows the marked separation of AII from AIII (Fig. 1A). Examination of the raw microarray data also revealed loss of *PGDS* expression in the glioblastoma group ($n = 11$; data not shown).

Quantitative PCR was used to quantify mRNA levels of *PGDS* in the differing grades of astrocytoma and normal brain controls. There was no significant difference in expression levels of *PGDS* in the AII specimens when compared with the normal brain controls. However, the expression of *PGDS* in the AIII and the GBM specimens were significantly reduced when compared with normal brain and AII, where levels were 2.5 and 5 times lower, respectively ($P = 0.013$; Fig. 1B).

Immunohistochemistry Analysis of PGDS and COX-2 Protein

Normal brain tissue displayed strong cytoplasmic immunostaining for *PGDS* (Allred score >2). All eight specimens from patients with an AII showed positive immunostaining (Allred score >2) for *PGDS* (Fig. 2A; Table 1). The percentage of positive tumors observed declined slightly as malignancy increased (Fig. 2B; Table 1). Among the 24 specimens from patients with AIII, 22 (92%) maintained moderate positive expression of *PGDS*, and among the 66 GBM specimens, 53 (80%) maintained moderate expression (Allred score 3-6). Although no significant difference was

observed (score categories of ≤ 2 or < 2 ; $P = 0.194$), a shift in the intensity of *PGDS* staining was noted, with a large proportion of AIII (42%) and GBM (42%) falling into the scoring category of 3 to 4, which is markedly weak and indicative of a reduction in protein expression (Table 1).

To determine if loss of *PGDS* expression was due to changes in protein in expression upstream, we measured all specimens for COX-2 expression. COX-2 protein expression was detected in normal brain neurons, and granular staining was observed in the cytoplasm of tumor cells in all astrocytoma specimens regardless of grade (Fig. 2C and D; Table 1). The percentage of positive COX-2 staining did not significantly differ between histologic grade with 6 of 8 (75%) AII, 17 of 24 (71%) AIII, and 51 of 64 (80%) GBM specimens, showing strong positive COX-2 staining ($P = 0.656$).

Multivariate Analysis and Patient Survival

A Cox proportional hazards regression model adjusted for age and stratified by tumor grades showed that a *PGDS* protein score of ≤ 2 was a strong predictor of poor survival ($P < 0.001$). The survival curves shown in Fig. 2E illustrate the effect of *PGDS* score on patient outcome. The mean survival for patients who scored >2 for *PGDS* was 4.16 years, which was significantly better than the mean survival for patients who scored ≤ 2 , which was 1.05 years ($P < 0.001$; Table 2).

Aberrant Methylation within the First Intron of PGDS

Because loss of *PGDS* expression in the high-grade brain tumor specimens is independent of COX-2 expression, we looked for alternate mechanisms of regulation. We designed primers sufficient to screen the entire coding sequence of *PGDS* using tumor DNA. No nucleotide alterations were identified in 18 GBM specimens.

Although there have been no previous reports of aberrant methylation of *PGDS*, we located a CpG island in intron 1 of the *PGDS* gene and designed primers to amplify this

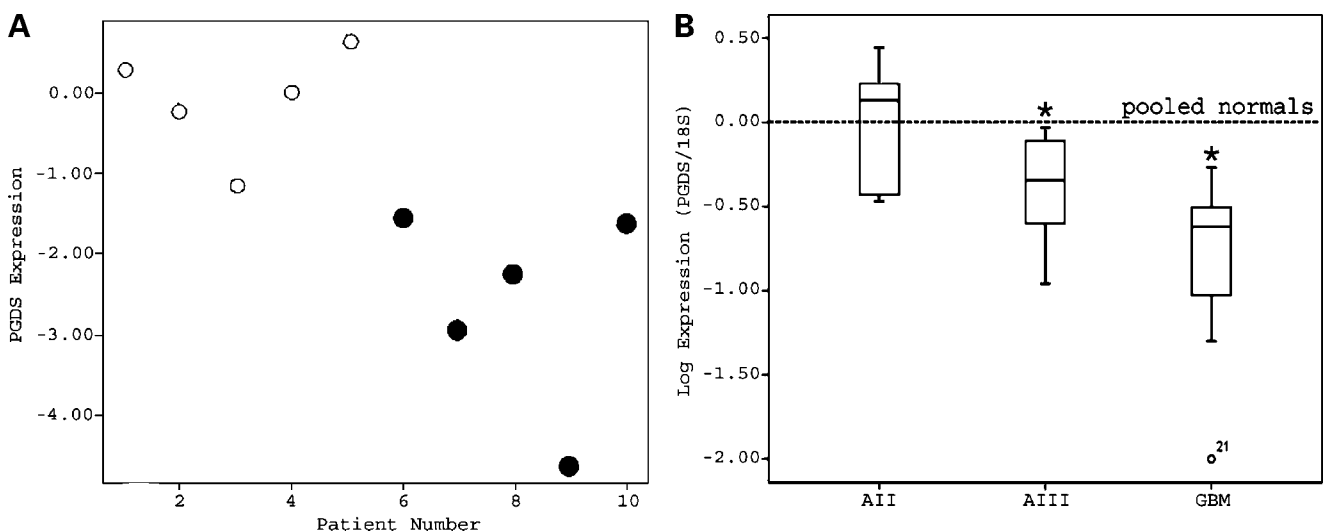


Figure 1. **A**, plot of normalized \log_2 *PGDS* gene expression results showing separation of the 5 AII tumors from the 6 AIII tumors. **B**, log-transformed box plot values for the quantitative PCR expression (normalized to the ribosomal 18S endogenous control) for each of the 5 AII, 8 AIII, and 14 GBM specimens after comparison with a pooled normal brain reference (broken horizontal line). *, $P < 0.005$; **, $P < 0.001$, Student's *t* test analysis.

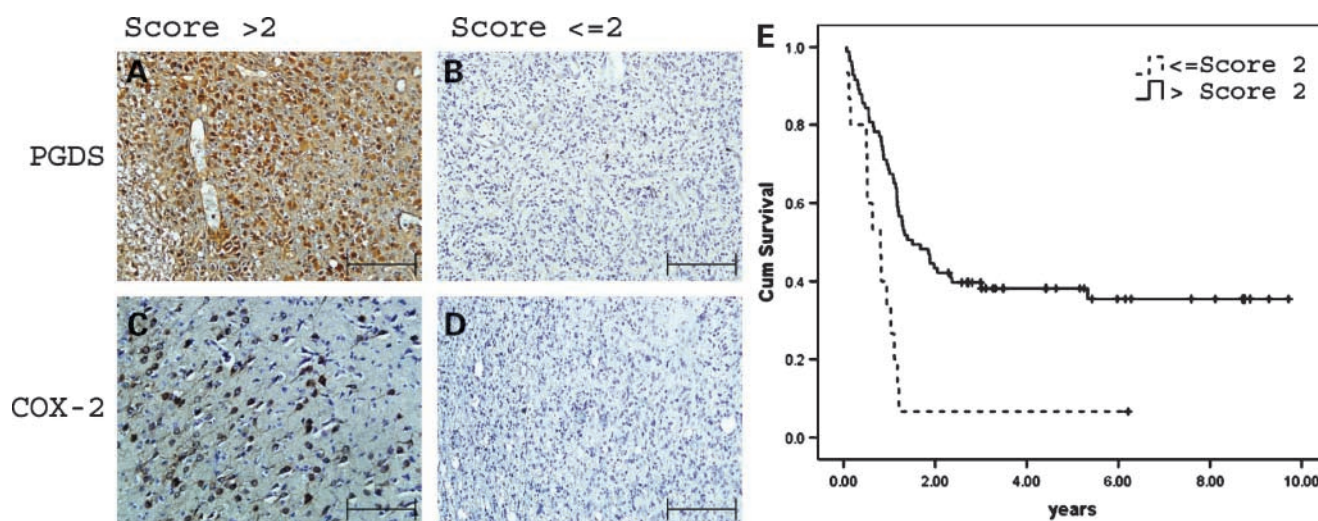


Figure 2. Immunohistochemistry expression and localization of PGDS and COX-2 in astrocytoma specimens. **A**, positive cytoplasmic PGDS staining in an AII specimen, representative of an Allred score of 6. **B**, weak PGDS staining in a GBM specimen, representative of an Allred score of 1. **C**, strong positive COX-2 staining in an AIII specimen, representative of an Allred score of 6. **D**, weak COX-2 staining in a AIII specimen, representative of an Allred score of 1. Bar, 100 μ m. **E**, disease-specific survival of patients with PGDS protein expression scores of ≤ 2 ($n = 15$) or > 2 ($n = 83$). Log-rank $P < 0.001$.

region. No CpG islands were detected within the promoter region. Within the 345-bp region, 32 CpG dinucleotides were identified and bisulfite sequencing was done. All tumor specimens (28 of 28) displayed some degree of methylation ranging from 3% to 41% (Fig. 3). From the methylation map, four regions of hypermethylation were observed: CpG 9 (72-73 bp), CpG 14-16 (129-138 bp), CpG 18 (166-167 bp), and CpG 32 (262-263 bp). These particular CpG dinucleotides were methylated in over 90% of samples. Using MatInspector,¹¹ putative transcription factors were found at each site and are summarized in Table 4. To further show that *PGDS* expression could be suppressed as a function of methylation, the A172 glioblastoma cell line, which showed 100% methylation and negligible expression of *PGDS* when measured with quantitative PCR, was treated with the demethylating agent 5-aza-deoxycytidine (1×10^{-6} mol/L) for 72 h and resulted in the significant induction of *PGDS* mRNA expression (data not shown).

Table 1. Summary of the immunohistochemistry staining scores for PGDS and COX-2

	Score ≤ 2 (%)	Score 3-4 (%)	Score 5-6 (%)	Score > 6 (%)	Total (%)
PGDS scoring					
AII	0 (0)	3 (37.5)	3 (37.5)	2 (25.0)	8 (100)
AIII	2 (8.3)	10 (41.7)	9 (37.5)	3 (12.5)	24 (100)
GBM	13 (19.7)	28 (42.4)	20 (30.3)	5 (7.6)	66 (100)
COX-2					
AII	2 (25.0)	4 (50.0)	2 (25.0)	0 (0)	8 (100)
AIII	7 (29.1)	12 (50.0)	4 (16.7)	1 (4.2)	24 (100)
GBM	13 (19.7)	30 (45.5)	21 (31.8)	2 (3.0)	66 (100)

PGD₂ Induces Growth Inhibition and Increases Sensitivity to COX-2 Pathway Inhibitors in the Glioblastoma Cell Line, A172

To elucidate whether the loss of *PGDS* in malignant AIII and GBM could be affecting tumor cell growth adversely, we used the A172 cell line as model for glioblastoma. PGD₂, which is produced by *PGDS*, was added to the A172 cells at an optimized concentration of 10^{-5} mol/L and cell proliferation and viability was measured at days 1 to 3 by MTS assay and trypan blue exclusion. At day 2, the proportion of viable cells proliferating decreased significantly by 40% after treatment with PGD₂ compared with untreated control cells ($P < 0.001$; Fig. 4A). A significant decrease in cell viability measured by trypan blue dye exclusion was also observed at day 2 in A172 cells treated with PGD₂ ($P < 0.001$; Fig. 4B).

We next examined the relative sensitivity of A172 cells to the COX-2-selective, nonsteroidal anti-inflammatory drugs, nimesulide and etodolac, and if the effect of these nonsteroidal anti-inflammatory drugs on cell proliferation and viability could be enhanced in the presence of PGD₂. Nimesulide and etodolac were added to A172 cells at an optimized concentration of 5×10^{-5} mol/L. At day 2, cell proliferation, measured by MTS, was significantly reduced by approximately 40% in cells treated with nimesulide ($P < 0.001$) and 35% in cells treated with etodolac ($P < 0.001$) when compared with untreated control cells. Cell viability, measured by trypan blue exclusion, was also significantly reduced in A172 cells treated with nimesulide ($P = 0.002$) and etodolac ($P = 0.002$; Fig. 4B).

When cells were cotreated with either of the COX-2 inhibitors (5×10^{-5} mol/L) plus PGD₂ (10^{-5} mol/L), reductions

¹¹ http://www.genomatix.de/cgi-bin/matinspector_prof/mat_fam

Table 2. Multivariate Cox regression analysis of PGDS score, tumor grade, and age

Variables	Relative risk (95% confidence interval)	P
Age	1.03 (1.01-1.05)	0.006
PGDS score	2.69 (1.43-5.04)	0.002
AII	—	0.000
AIII	0.106 (0.01-0.81)	0.031
GBM	0.06-0.42	0.000

in cell proliferation and viability were significantly greater than treatment with a single agent ($P = 0.002$). The cotreatment of PGD₂ and nimesulide resulted in a 60% reduction in cell proliferation ($P = 0.002$), whereas the combination of PGD₂ with etodolac resulted in a 55% reduction in cell proliferation ($P = 0.002$) when compared with untreated cells measured at day 2 (Fig. 4A). Similar trends were observed when cell viability was measured with trypan blue (Fig. 4B).

To ascertain if the cell death induced by PGD₂ alone and in combination with the COX-2 inhibitors was by an

apoptotic mechanism, TUNEL staining was carried out at days 1 to 3. No TUNEL-positive cells were observed in any of the treatments at any time point.

Discussion

Ten years ago, PGDS, also called β-trace protein, was reported to be a potentially useful marker for brain tumors (18). Levels of PGDS were significantly lower in the cerebrospinal fluid from patients diagnosed with a brain tumor when compared with normal individuals (18). Reduced levels of PGDS have been associated with increased malignancy in other cancers, particularly in ovarian cancer cells (19, 20) and in the premalignant stages of oral epithelia (21). We also observed an inverse association between mRNA and protein expression levels of PGDS with astrocytoma malignancy. For the very first time, we showed that low PGDS protein expression (score ≤ 2), when used in conjunction with tumor grade and adjusted for age, identified a group of patients whose prognosis was poor.

PDGS is the main arachidonic acid metabolite produced in neurons and glial cells of the central nervous system. PGDS is bifunctional: it mediates the final regulatory step of PGD₂ biosynthesis and acts as a retinoid transporter (19).

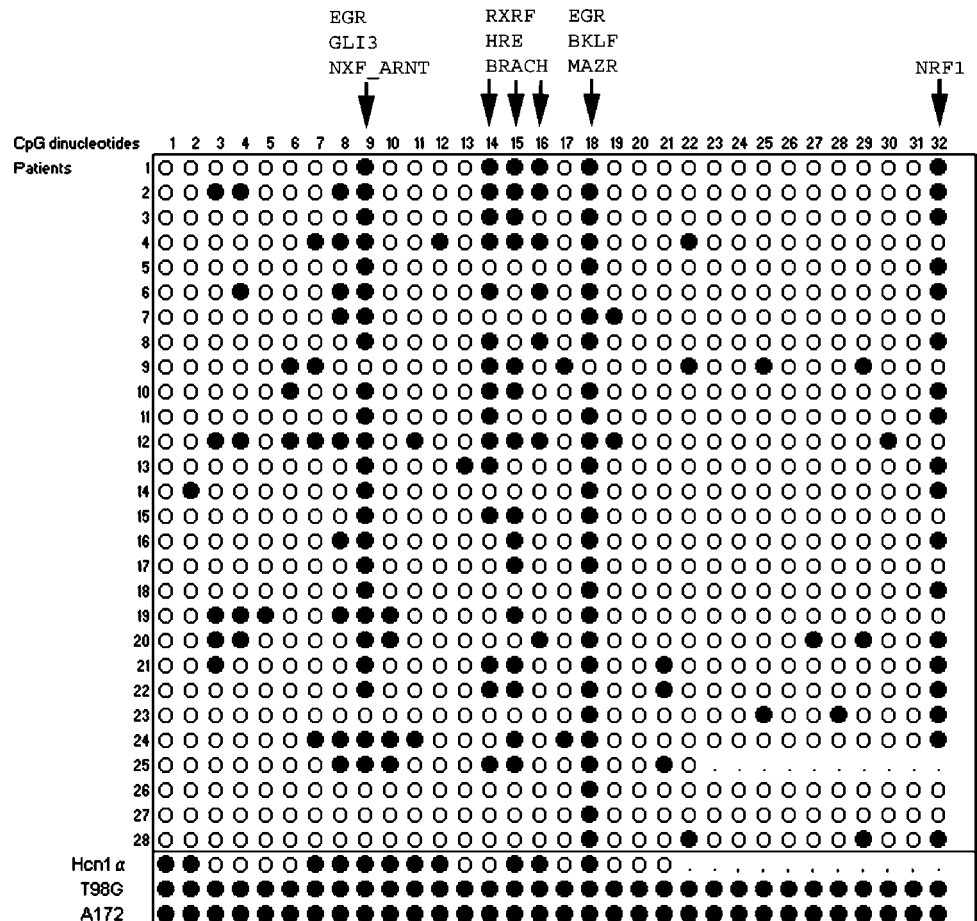


Figure 3. Methylation status of the 345-bp region of intron 1 of the PGDS gene. Line, sample; circle, CpG dinucleotide. Open circles, unmethylated dinucleotides; filled circles, methylated dinucleotides. Period, area of a sequence that could not be deciphered. Arrows, putative binding sites within the hypermethylated regions between 72 and 263 bp.

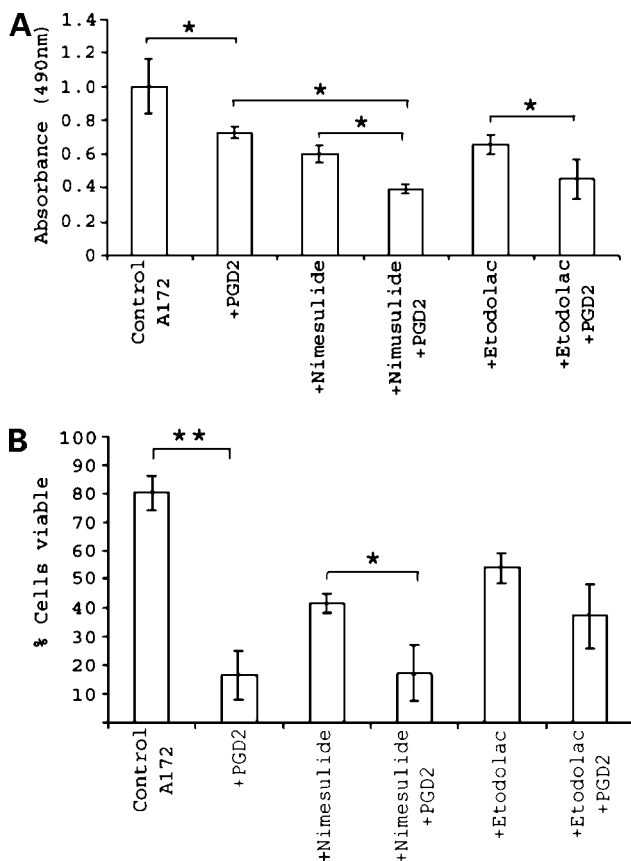


Figure 4. Cell proliferation and viability studies. **A**, day 2 of MTS assay for A172 cells treated with PGD₂ (10^{-5} mol/L), nimesulide (5×10^{-5} mol/L), etodolac (5×10^{-5} mol/L), or combinations of PGD₂ with either nimesulide or etodolac. Mean \pm SD of three experiments. Absorbance (Y axis) was measured at 492 nm ($A_{492-650}$). **B**, day 2 of trypan blue exclusion assay for A172 cells treated with PGD₂ (10^{-5} mol/L), nimesulide (5×10^{-5} mol/L), etodolac (5×10^{-5} mol/L), or combinations of PGD₂ with either nimesulide or etodolac. Mean \pm SD of three experiments. Percentage viable cells that did not absorb the trypan blue dye (Y axis) was derived from counting cells on a hemocytometer. *, $P < 0.005$; **, $P < 0.001$, Student's *t* test analysis.

Once PGD₂ and its metabolites are made, they are involved in multiple physiologic events, including the regulation of sleep and ocular pressure (22–24), body odor, pain response and body temperature control (25), prevention of platelet aggregation (26), and induction of vasodilation (27). The final metabolites of PGD₂ also have potent antiproliferative activity on tumor cells (28, 29).

We observed significant reductions in cell proliferation and viability in the A172 glioblastoma cell line when PGD₂ was exogenously supplied. The metabolite, 15-deoxy- $\Delta^{12,14}$ -prostaglandin J₂, isolated from normal prostate stromal cells, slowed the growth and induced partial differentiation of prostate cancer cells when administered (30). It is thought that PGD₂ and its other metabolites like 15-deoxy- $\Delta^{12,14}$ -prostaglandin J₂ exert their cell death effect through the peroxisome proliferator-activated receptor γ (30). Previous studies have documented high expression

levels of peroxisome proliferator-activated receptor γ in high-grade brain tumors (31) as well as in the A172 cell line that we used for our *in vitro* studies (32). Interestingly, when PGD₂ was added to A172 cells, the observed cell death was not mediated through the apoptotic pathway. Although we only used one measure of apoptosis, TUNEL, this observation was consistent with the studies by Banerjee et al. (21).

We showed that protein expression of COX-2 was abundant in all astrocytomas regardless of grade. Aberrant expression of COX-2 has been widely reported as a key player involved in cancer-related inflammation and progression (33). Specific inhibitors of COX-2 have been shown to be very effective in impairing human glioma cell line growth *in vitro* and intracranial inhibition in rat *in vivo* models. In our *in vitro* experiments, we used the COX-2 inhibitors, nimesulide and etodolac, and showed a substantial inhibitory effect on cell proliferation rates and cell viability. However, when either of the COX-2 inhibitors was applied in combination with PGD₂, the efficacy was significantly improved. COX-2 inhibitors possess very few side effects and are increasingly used as additive compounds to enhance other chemotherapies such as low-dose temozolomide (34) or in combination with retinoic acid rather than as a single-agent therapy (35). PGD₂ is known to act as a negative feedback regulator of COX-2 gene transcription; thus, the introduction of a PGD₂-like analogue such as ZK 118.182 (36) and its analogue AL-6556;13,14-dihydro-2K118182 (37) and TS-002 (38) may improve the utility of COX-2 inhibitors (39).

We showed that PGDS was significantly repressed at both gene and protein levels in malignant astrocytomas but not in AII and normal brain. Reduced PGDS protein expression significantly correlated with poorer survival outcome when patients were stratified by tumor grade. It is critical to uncover the mechanism(s) that could lead to PGDS dysregulation during the latter stages of tumor progression. Although COX-2 activity is a rate-limiting enzyme in prostanoid synthesis, no correlation between low PGDS and low COX-2 protein expression could be shown using immunohistochemistry. Thus, our attention shifted to looking for significant gene alterations such as insertion, deletion, rearrangement, or point mutations that could therefore result in loss of PGDS gene expression and post-translational changes in protein expression.

PGDS is located on the chromosomal arm, 9q34.2-34.3. Loss of heterozygosity is a common mechanism to result in structural genomic alteration and loss of expression of genes with tumor-suppressing properties. However, a loss of heterozygosity study of 18 AII and 26 AIII specimens showed that the loss of chromosome 9q was an infrequent occurrence, with loss of heterozygosity of 9q recorded in only one specimen (AII; ref. 40). We examined and screened the 6 exons of PGDS for mutations; however, none were observed in any of the GBM despite low mRNA and/or protein expression of PGDS.

Despite no detectable mutations, for the first time we provide evidence of a hypermethylated region within

intron 1 of the *PGDS* gene. Transcriptional silencing of this gene could be reversed using a demethylation treatment. On mapping the areas of methylation, four areas of hypermethylation were evident. Numerous putative binding sites were identified within the four regions including the GLI zinc finger family, which have been implicated in medulloblastoma formation (41) and hedgehog signaling (42) and the transcription factor *early growth response-1*, which can be induced by retinoic acid through the extracellular signal-regulated kinase 1/2 pathway and has been postulated to play a role in neuronal differentiation (43). The *retinoid X receptor* heterodimer ligand was also identified as a candidate binding partner within the *PGDS* hypermethylation region. Peroxisome proliferator-activated receptor γ is a permissive retinoid X receptor heterodimer partner (44). Coupled with evidence provided earlier that cell death induced by PGD_2 is mediated through the peroxisome proliferator-activated receptor γ ligand, it is tantalizing to suggest that hypermethylation of this region could be contributing to tumorigenesis and a reduction in cell death in malignant glioma.

In conclusion, we have shown that loss of *PGDS* is a significant biological event involved in the malignant progression of astrocytomas and is predictive of poor overall survival. *In vitro*, we provide evidence for PGD_2 substitution to enhance the efficacy of COX-2 inhibitors. This finding has exciting implications for early interventional efforts for the grade 2 and 3 astrocytomas. Anti-inflammatory PGD_2 -like analogues may help prevent or delay the malignant progression in astrocytoma.

Disclosure of Potential Conflicts of Interest

No potential conflicts of interest were disclosed.

Acknowledgments

We thank Karen Byth-Wilson for statistical analysis.

References

- Louis DN, Ohgaki H, Wiestler OD, et al. The 2007 WHO classification of tumours of the central nervous system. *Acta Neuropathol* 2007;114:97–109.
- Buckner JC. Factors influencing survival in high-grade gliomas. *Semin Oncol* 2003;30:10–4.
- Watanabe K, Tachibana O, Yonekawa Y, et al. Role of gemistocytes in astrocytoma progression. *Lab Invest* 1997;76:277–84.
- Martins DC, Malheiros SM, Santiago LH, et al. Gemistocytes in astrocytomas: are they a significant prognostic factor? *J Neurooncol* 2006;80:49–55.
- Stander M, Peraud A, Leroch B, et al. Prognostic impact of TP53 mutation status for adult patients with supratentorial World Health Organization grade II astrocytoma or oligoastrocytoma: a long-term analysis. *Cancer* 2004;101:1028–35.
- Ohgaki H. Genetic pathways to glioblastomas. *Neuropathology* 2005;25:1–7.
- Peraud A, Kreth FW, Wiestler OD, et al. Prognostic impact of TP53 mutations and p53 protein overexpression in supratentorial WHO grade II astrocytomas and oligoastrocytomas. *Clin Cancer Res* 2002;8:1117–24.
- Houillier C, Lejeune J, Benouaich-Amiel A, et al. Prognostic impact of molecular markers in a series of 220 primary glioblastomas. *Cancer* 2006;106:2218–23.
- Mott RT, Turner KC, Bigner DD, et al. Utility of EGFR and PTEN numerical aberrations in the evaluation of diffusely infiltrating astrocytomas. Laboratory investigation. *J Neurosurg* 2008;108:330–5.
- Varela M, Ranuncolo SM, Morand A, et al. EGF-R and PDGF-R, but not bcl-2, overexpression predict overall survival in patients with low-grade astrocytomas. *J Surg Oncol* 2004;86:34–40.
- Huang H, Colella S, Kurrer M, et al. Gene expression profiling of low-grade diffuse astrocytomas by cDNA arrays. *Cancer Res* 2000;60:6868–74.
- Heimberger AB, McGary EC, Suki D, et al. Loss of the AP-2 α transcription factor is associated with the grade of human gliomas. *Clin Cancer Res* 2005;11:267–72.
- McDonald KL, O'Sullivan MG, Parkinson JF, et al. IQGAP1 and IGFBP2: valuable biomarkers for determining prognosis in glioma patients. *J Neuropathol Exp Neurol* 2007;66:405–17.
- Allred DC, Harvey JM, Berardo M, et al. Prognostic and predictive factors in breast cancer by immunohistochemical analysis. *Mod Pathol* 1998;11:155–68.
- Parkinson JF, Wheeler HR, Clarkson A, et al. Variation of *O*(6)-methylguanine-DNA methyltransferase (MGMT) promoter methylation in serial samples in glioblastoma. *J Neurooncol* 2008;87:71–8.
- Elston MS, Gill AJ, Conaglen JV, et al. Wnt pathway inhibitors are strongly down-regulated in pituitary tumors. *Endocrinology* 2008;149:1235–42.
- Foltz G, Ryu GY, Yoon JG, et al. Genome-wide analysis of epigenetic silencing identifies BEX1 and BEX2 as candidate tumor suppressor genes in malignant glioma. *Cancer Res* 2006;66:6665–74.
- Saso L, Leone MG, Sorrentino C, et al. Quantification of prostaglandin D synthetase in cerebrospinal fluid: a potential marker for brain tumor. *Biochem Mol Biol Int* 1998;46:643–56.
- Malki S, Bibeau F, Notarnicola C, et al. Expression and biological role of the prostaglandin D synthase/SOX9 pathway in human ovarian cancer cells. *Cancer Lett* 2007;255:182–93.
- Su B, Guan M, Zhao R, et al. Expression of prostaglandin D synthase in ovarian cancer. *Clin Chem Lab Med* 2001;39:1198–203.
- Banerjee AG, Bhattacharyya I, Vishwanatha JK. Identification of genes and molecular pathways involved in the progression of premalignant oral epithelia. *Mol Cancer Ther* 2005;4:865–75.
- Hayaishi O, Urade Y, Eguchi N, et al. Genes for prostaglandin D synthase and receptor as well as adenosine A2A receptor are involved in the homeostatic regulation of nrem sleep. *Arch Ital Biol* 2004;142:533–9.
- Barcelo A, de la Pena M, Barbe F, et al. Prostaglandin D synthase (β trace) levels in sleep apnea patients with and without sleepiness. *Sleep Med* 2007;8:509–11.
- Urade Y, Hayaishi O. Prostaglandin D₂ and sleep regulation. *Biochim Biophys Acta* 1999;1436:606–15.
- Eguchi N, Minami T, Shirafuji N, et al. Lack of tactile pain (allodynia) in lipocalin-type prostaglandin D synthase-deficient mice. *Proc Natl Acad Sci U S A* 1999;96:726–30.
- Rajtar G, Cerletti C, Castagnoli MN, et al. Prostaglandins and human platelet aggregation. Implications for the anti-aggregating activity of thromboxane-synthase inhibitors. *Biochem Pharmacol* 1985;34:307–10.
- Kamanna VS, Kashyap ML. Nicotinic acid (niacin) receptor agonists: will they be useful therapeutic agents? *Am J Cardiol* 2007;100:S53–61.
- Fukushima M, Sasaki H, Fukushima S. Prostaglandin J₂ and related compounds. Mode of action in G₁ arrest and preclinical results. *Ann N Y Acad Sci* 1994;744:161–5.
- Sasaki H, Fukushima M. Prostaglandins in the treatment of cancer. *Anticancer Drugs* 1994;5:131–8.
- Kim J, Yang P, Suraokar M, et al. Suppression of prostate tumor cell growth by stromal cell prostaglandin D synthase-derived products. *Cancer Res* 2005;65:6189–98.
- Kato M, Nagaya T, Fujieda M, et al. Expression of PPAR γ and its ligand-dependent growth inhibition in human brain tumor cell lines. *Jpn J Cancer Res* 2002;93:660–6.
- Morosetti R, Servidei T, Mirabella M, et al. The PPAR γ ligands PGJ₂ and rosiglitazone show a differential ability to inhibit proliferation and to induce apoptosis and differentiation of human glioblastoma cell lines. *Int J Oncol* 2004;25:493–502.

33. Wang MT, Honn KV, Nie D. Cyclooxygenases, prostanoids, and tumor progression. *Cancer Metastasis Rev* 2007;26:525–34.
34. Tuettenberg J, Grobholz R, Korn T, et al. Continuous low-dose chemotherapy plus inhibition of cyclooxygenase-2 as an antiangiogenic therapy of glioblastoma multiforme. *J Cancer Res Clin Oncol* 2005;131:31–40.
35. Levin VA, Giglio P, Puduvalli VK, et al. Combination chemotherapy with 13-*cis*-retinoic acid and celecoxib in the treatment of glioblastoma multiforme. *J Neurooncol* 2006;78:85–90.
36. Pons F, Williams TJ, Kirk SA, et al. Pro-inflammatory and anti-inflammatory effects of the stable prostaglandin D₂ analogue, ZK 118.182. *Eur J Pharmacol* 1994;261:237–47.
37. Sharif NA, Williams GW, Crider JY, et al. Molecular pharmacology of the DP/EP2 class prostaglandin AL-6598 and quantitative autoradiographic visualization of DP and EP2 receptor sites in human eyes. *J Ocul Pharmacol Ther* 2004;20:489–508.
38. Yamada K, Hasegawa M, Kametani S, et al. Nose-to-brain delivery of TS-002, prostaglandin D₂ analogue. *J Drug Target* 2007;15:59–66.
39. Wang C, Fu M, D'Amico M, et al. Inhibition of cellular proliferation through I κ B kinase-independent and peroxisome proliferator-activated receptor γ -dependent repression of cyclin D1. *Mol Cell Biol* 2001;21:3057–70.
40. von Deimling A, Bender B, Jahnke R, et al. Loci associated with malignant progression in astrocytomas: a candidate on chromosome 19q. *Cancer Res* 1994;54:1397–401.
41. Kimura H, Stephen D, Joyner A, et al. Gli1 is important for medulloblastoma formation in Ptc1 +/- mice. *Oncogene* 2005;24:4026–36.
42. Szczepny A, Hime GR, Loveland KL. Expression of hedgehog signalling components in adult mouse testis. *Dev Dyn* 2006;235:3063–70.
43. Lee YS, Jang HS, Kim JM, et al. Adenoviral-mediated delivery of early growth response factor-1 gene increases tissue perfusion in a murine model of hindlimb ischemia. *Mol Ther* 2005;12:328–36.
44. Li D, Yamada T, Wang F, et al. Novel roles of retinoid X receptor (RXR) and RXR ligand in dynamically modulating the activity of the thyroid hormone receptor/RXR heterodimer. *J Biol Chem* 2004;279:7427–37.